

## Research Paper

# Feasibility of Using Wavelet Analysis and Machine Learning Method in Technical Diagnosis of Car Seats

Cezary BARTMAŃSKI, Alicja BRAMORSKA\*

*Department of Acoustics, Electronics and IT Solutions Central Mining Institute  
National Research Institute  
Katowice, Poland*

\*Corresponding Author e-mail: [abramorska@gig.eu](mailto:abramorska@gig.eu)

(received October 24, 2023; accepted June 10, 2024; published online August 27, 2024)

This paper presents the results of preliminary research aimed at developing a method for rapid, non-contact diagnostics of the electric drive of car seats. The method is based on the analysis of acoustic signals produced during the operation of the drive. Pattern recognition and machine learning processes were used in the diagnosis. A method of feature extraction (diagnostic symptoms) using wavelet decomposition of acoustic signals was developed. The discriminative properties of a set of diagnostic symptoms were tested using the “Classification Learner” application available in MATLAB. The obtained results confirmed the usefulness of the developed method for the technical diagnostics of car seats.

**Keywords:** acoustic diagnostics; wavelet decomposition; machine learning.



Copyright © 2024 The Author(s).  
This work is licensed under the Creative Commons Attribution 4.0 International CC BY 4.0  
(<https://creativecommons.org/licenses/by/4.0/>).

## 1. Introduction

The subject of this study is the mechanical construction of a car seat with a driving device allowing to change the angle of the seat backrest. The device consists of an electric motor and a gearbox (Fig. 1) and is a compact module without the possibility of disassembling it, for example, for repair. In the event of failure or malfunction, the manufacturer replaces the entire module.

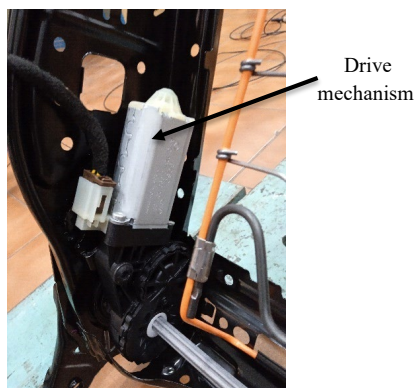


Fig. 1. Appearance of the drive mechanism of a car seat.

The main goal of the research is to develop a quick method for diagnosing the seat construction at the production stage. Due to the postulated speed of diagnosis and the small size of the drive device, it is decided to look for a solution based on the analysis of acoustic signals generated by the operating drive device. This choice is justified due to the generally well-known high content of relevant information about the state of the object in the acoustic signal generated during its operation (BASZTURA, 1996; LIN, 2001; GŁOWACZ, 2014; PAWLIK, 2019).

The starting point for the study was a small batch of seats (11 pieces) supplied by the manufacturer. Some of the seats were marked as good (meeting the manufacturer's requirements) and the rest as defective. According to the manufacturer's requirements, diagnostics of subsequent batches of seats should categorize them into two classes: good (technically efficient) and bad (defective) without identifying the specific defective component. The problem presented here falls under a topic referred to in literature as pattern recognition. It deals with the recognition of the affiliation of various objects to certain predefined classes. Objects within each class may differ more or less from each

other, and the number of objects within each class can be any.

The pattern recognition process is divided into two parts called feature extraction and classification. In the first part, characteristic features are extracted from the measured signal. In the second part, calculations are performed on the set of these features using the information contained in the so-called learning sequence. A learning sequence is a previously prepared set of features representing objects for which the correct classification is known. As a result of these calculations, a decision is made as to which class the recognized object belongs to (DUDA, HART, 1973; SUN *et al.*, 2004; XI *et al.*, 1997).

## 2. Test stand and measurement database

The work is performed on a test stand used in the laboratory for measuring the sound power level of mechanical equipment, which was adapted to the needs of the present work (Fig. 2).

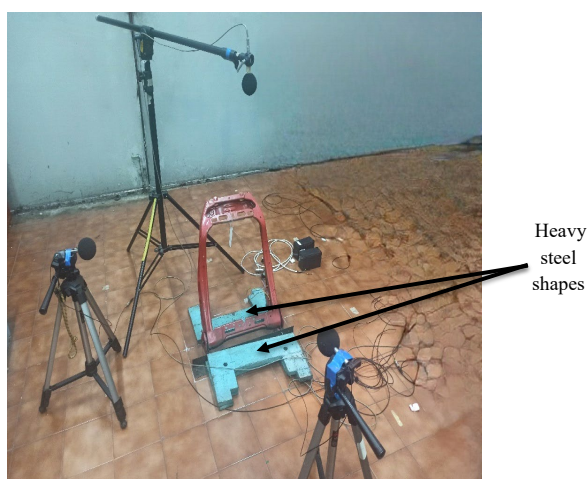


Fig. 2. View of test stand.

The stand is located in a laboratory hall measuring  $9.3 \text{ m} \times 7 \text{ m} \times 5.2 \text{ m}$ . The hall has smooth walls and a floor covered with ceramic tiles to reflect acoustic waves. The room is partially filled with laboratory furniture. Following the guidelines in Annex A of (International Organization for Standardization, 2010), the mentioned test environment was classified as a rectangular industrial room with an average sound absorption coefficient of  $a = 0.15$ .

The seat structure is fixed to the floor by loading the seat base with two heavy steel fittings, ensuring its immobilization during testing (Fig. 2). In the initial stage of testing, microphones mounted on measurement stands were placed at the vertices and in the center of the walls of the virtual cuboid surrounding the test object – a total of 9 measurement points were established (Fig. 3). The dimensions of the cuboid were chosen so that the distance from the walls to the test

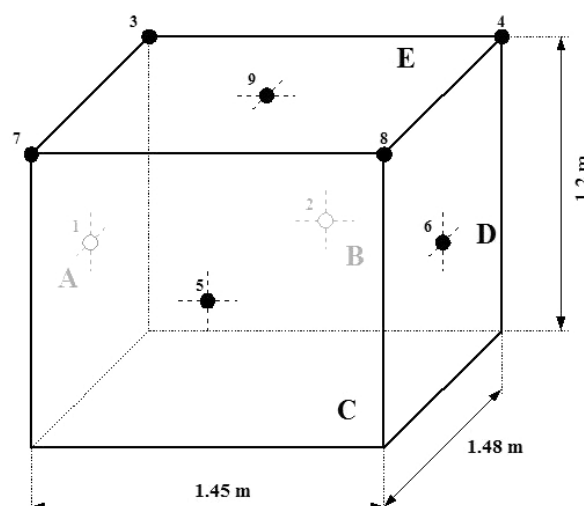


Fig. 3. Arrangement of microphones on test bench.

object was 0.5 m. The individual microphones were oriented so that their axes:

- were perpendicular to the measurement plane for measurement points no. 1, 2, 5, 6, and 9;
- indicated the point of intersection of the diagonals of the perpendicular for measurement points no. 3, 4, 7, and 8.

The small distance, compared to the size of the hall, minimizes the influence of the reflected wave on the recorded signal. Nevertheless, it should be noted that in the case of the presented research, it is not important to determine the exact value of the sound pressure level, but rather to determine the interrelationships of the different parts of the signal spectrum, as will be discussed later in the article.

The acoustic signal was recorded during the operation of the driving device for two directions of seat backrest movement: forward and backward. The time of backrest movement between extreme positions was approximately 20 s. The signals were recorded on a PULSE digital recorder, manufactured by Brüel & Kjær. The time courses of these signals and their measured features allow them to be classified, in accordance with the systematics used in the literature on signal analysis, as transient non-stationary signals (PIERSOL, 1989; SZABATIN, 2000). An example of the time course of the recorded signals is shown in Fig. 4.

Measurements of the acoustic background noise in the hall indicate that the S/N ratio of the recorded acoustic signals was more than 13 dB. This testifies to the negligible influence of the acoustic background noise on the signal under study.

It is necessary to ensure that the acoustic environment at the future location of the manufacturer's diagnostic station is comparable to the current one.

Initially, the signals were recorded in the acoustic range up to 20 kHz. Frequency analysis indicates that

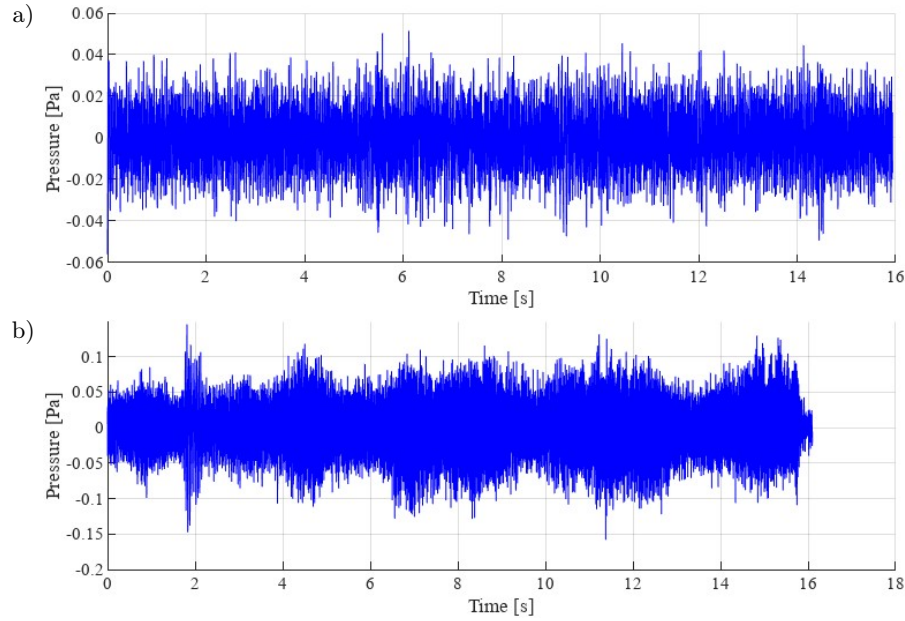


Fig. 4. Time course of the acoustic signal generated by the seat drive device: a) technically efficient seat; b) defective seat.

the spectra of these signals are dominated by components in the range of 20 Hz–60 Hz, and the maximum frequency practically does not exceed 200 Hz. Figure 5 shows an example of the spectra of the signals generated by the technically efficient and defective seats, respectively. Unfortunately, it was found that in each case, the differences of the spectra are not as clear as illustrated in the figures. Differences were also observed in the spectra of the signals generated for different directions of backrest movement for both the technically efficient and defective seats.

Measurements were made on all 11 seats – 5 seats marked as good and 6 seats marked as not meeting the

manufacturer's requirements. The recordings of measured signals, in the form of samples of instantaneous values, constituted the measurement database for the further part of the work.

The levels of signals recorded at particular points of the grid did not differ significantly; however, at measurement points 1, 2, and 5 (at the height of  $h = 0.60$  m) this level was higher. Finally, for the planned future measurements, one point of microphone installation was selected, i.e., point 5, located near the drive mechanism of a seat, and for the recordings made at this point further signal processing and calculations were performed.

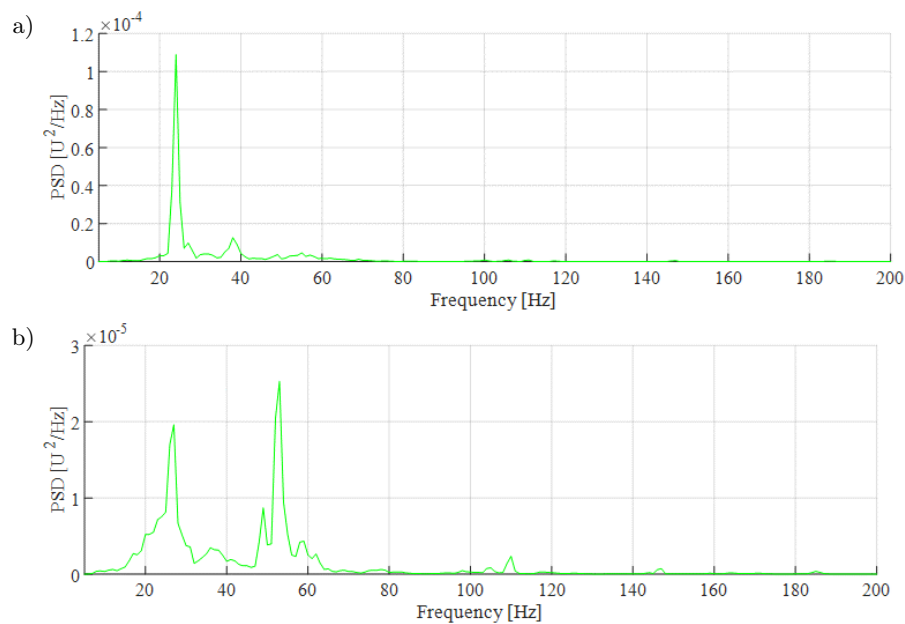


Fig. 5. Acoustic signal spectrum: a) technically efficient seat; b) defective seat.

### 3. Feature extraction

Vibroacoustic signals produced during the operation of mechanical equipment carry important information about the dynamic processes within them. Therefore, the analysis of vibroacoustic signals is one of the most important methods used in condition monitoring and technical diagnostics of equipment.

In practice, many methods of signal analysis, e.g., FFT, STFT, Wigner-Ville distribution are used in this area (TANG *et al.*, 2010). Among these, wavelet analysis is currently one of the most advanced tools of signal analysis, confirmed by numerous practical applications. It covers almost all aspects of technical diagnostics of mechanical equipment, including time-frequency analysis of signals, fault feature extraction, singularity detection for signals, denoising and extraction of weak signals, compression of signals, and system identification (BATKO *et al.*, 2005; HAN *et al.*, 2022; TANG *et al.*, 2010; PENG, CHU, 2004; LIN, QU, 2000; STASZEWSKI, 1998; HUANG, SOLORZANO, 1971; YANG *et al.*, 2022).

The review of the results of the spectral analysis of the acoustic signals produced by the working seat drive device indicates that there are differences in the spectra between the objects marked, according to the manufacturer's criteria, as good and bad. However, there are also differences between both good and bad objects.

The aim of processing recorded acoustic signals is to extract information about the individual characteristics of particular signals contained in their spectrum. In the discussed situation, it concerns the information allowing to make a decision about the technical condition of the tested object.

As the basic idea of creating the feature vector, we have established the development of a discrete representation of the acoustic signal into a functional series, followed by the separation of components of this expansion that carry significant energy of the signal. Coefficients of the selected components of this expansion will constitute the components of the feature vector (PENG, CHU, 2004).

In this paper, it was decided to use the method of wavelet analysis of signals to implement the feature extraction process. The basis of this analysis is the decomposition of the signal based on a set of orthogonal basis functions, called wavelets. The set of basis functions is generated by scaling and shifting the so-called mother wavelet in the time domain. The decomposition allows the signal to be represented as a superposition of wavelets. The coefficients of this superposition, called wavelet coefficients, are determined by the wavelet transform of the signal. The values of the wavelet coefficients measure the degree of correlation between the signal and the wavelet, making the proper choice of wavelet type crucial.

The values of the components of the feature vectors are a function of the type of wavelet selected for analysis. The purpose of selecting a particular wavelet is to obtain the strongest possible correlation between the signal with a small number of basis wavelets. As mentioned earlier, the values of wavelet coefficients are a measure of the degree of correlation between the wavelet and the signal.

The selection of the wavelet was done experimentally. A test was performed by decomposing the recorded signals using different wavelets and selecting the wavelet showing the highest degree of correlation with the signal. The parameter to be evaluated in this experiment was chosen as the maximum value of the modulus of the wavelet coefficients for each level of decomposition, according to the formula:

$$cDk_{\text{MAX}} = \max_{\{d_k\}} |d_k[i]|, \quad (1)$$

where  $k$  is the decomposition level index,  $i$  is the index of the element in the sequence of wavelet coefficients,  $d_k[i]$  is the sequence of coefficients at the  $k$ -th decomposition level.

The wavelets from the Daubechie, Symlet, and Coiflet families were examined. In light of these studies, no specific wavelet type was found to be particularly advantageous for the feature extraction process. However, several wavelets performed favorably in this regard. For this reason, further studies were limited to two wavelets, i.e., db10 and sym7.

A key challenge in the effectiveness of the diagnostics is the correct selection of features and their number, which determines the structure of the feature vector. A review of the literature on the subject indicates that there are many ways to optimize the process of feature selection. It is worth mentioning the main approaches for solving this problem. These include: thresholding methods, using wavelet entropy to optimize parameters of the wavelet function, selecting the proper coefficients using statistical criteria, employing wavelet packet coefficients as features, and using principal component analysis (PCA) to reduce the size of the feature space extracted from wavelet coefficients (BIAŁASIEWICZ, 2004; PENG, CHU, 2004; SYED, MURALIDHARAN, 2022; QIU *et al.*, 2006; DING *et al.*, 2023).

For the sake of completeness, it is worth noting that the above-mentioned method of feature extraction based on wavelet coefficient selection does not exhaust the possibilities offered by wavelet analysis of signals. Other methods mentioned in the literature, which are not the subject of this paper, can be classified as: wavelet energy-based, singularity-based, and wavelet function-based methods, etc. (PENG, CHU, 2004).

In the classical wavelet analysis method, the signal is decomposed into two lower-resolution representations of the signal: a detailed representation

and a coarse representation (signal approximation). The coarse representation can also be represented as the sum of the detailed and coarse representations from the previous resolution level. Thus, the detailed representation at a given resolution level does not change after each subsequent decomposition step, while the sequence of detailed representations, which characterize the analyzed signal, increases by one element (Fig. 6).

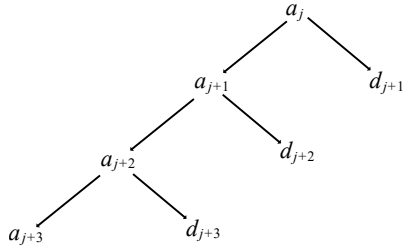


Fig. 6. Multiresolution signal decomposition scheme for three resolution levels.

The signal separation operation, which is a single level of wavelet decomposition from a signal of a given resolution level, is equivalent to its filtering by a set of digital quadrature low-pass and high-pass filters, and a subsequent downsampling operation (Fig. 7).

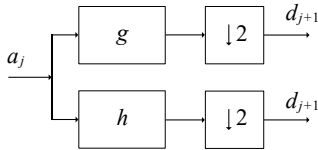


Fig. 7. Single level signal decomposition:  $h$  – low pass filter;  $g$  – high pass filter;  $\downarrow 2$  – decimation symbol.

The result of low-pass filtering is a sequence of samples that is the coarse approximation of the signal ( $a_i$ ), while the result of high-pass filtering is a sequence of samples representing the details of the signal ( $d_i$ ) at the immediately lower resolution level. Decimation, which involves removing every second sample from the resulting sample sequences at the output of the filters, prevents the introduction of redundant information into these sequences. The described iterative algorithm for determining the discrete wavelet transform (defined for discrete values of scale and shift parameters) is named, after its creator, the Mallat algorithm (MALLAT, 1989).

A decomposition of the signals up to level 8 resolution was performed. The components of the feature vector  $\mathbf{x}$  were computed from a sequence of wavelet coefficients of individual level decompositions. The individual components of the feature vector contain information about individual features of the signal, contained in a specific frequency range resulting from the division of the band into halves in subsequent stages of the decomposition of the analyzed signal (Fig. 8).

Considering the bandwidth of the measurement path for the acoustic signals, the decomposition components labeled D7 and D8 were excluded, as they fall outside the measurement bandwidth. Finally, the number of components in the feature vector, and thus the dimension of the feature space is  $n_{wt} = 6$ . The bandwidths of the decomposition components at the selected resolution levels, from which the individual components of the feature vectors were calculated, are shown in Table 1.

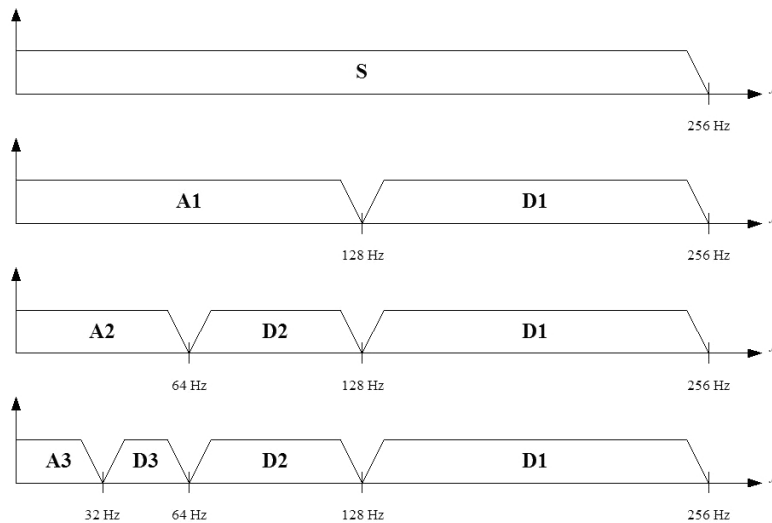


Fig. 8. Division of the signal band as a result of signal decomposition.

Table 1. Bandwidth of selected signal decomposition components.

Feature vector component	1	2	3	4	5	6
Component designation	D6	D5	D4	D3	D2	D1
Frequency range $f$ [Hz]	4–8	8–16	16–32	32–64	64–128	128–256



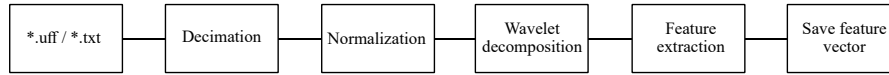


Fig. 9. Block diagram of the process of creating a feature vector.

The feature vector component value was defined as the root mean square (RMS) value of the reconstructed decomposition components based on the sequence of wavelet coefficients at a given decomposition level:

$$x_j = \sqrt{\frac{1}{N_k} \cdot \sum_{i=1}^{N_k} (d_k[i])^2}, \quad (2)$$

where  $j$  – the designation of the component of the feature vector,  $k$  – the decomposition level indicator,  $N_k$  – the number of wavelet coefficients for the  $k$ -th decomposition level, and  $d_k[i]$  – the  $i$ -th wavelet coefficient of the  $k$ -th decomposition level.

Feature extraction is only one, but nevertheless an essential, component of the feature vector creation process. The entire process is shown in Fig. 9.

Files downloaded from the recorder (\*.uff), containing samples of instantaneous values of the acoustic signal are processed into format suitable for MATLAB (\*.txt). The sampling frequency during recording was  $f_s = 65536$  Hz. This value was chosen during the preliminary research stage for problem recognition. Considering the found spectrum of the studied acoustic signals, this frequency can be significantly reduced, which allows for a decrease in the size of the registration files without losing the information contained in the spectrum. The recordings were resampled (decimated) to a sampling frequency of  $f_{s\_res} = 512$  Hz. After normalizing the signal energy, the recordings are subjected to wavelet decomposition as described above, and the feature vector values are calculated from the obtained sample sequences.

In classical wavelet analysis of signals, one should pay attention to high bandwidth of most decomposi-

tion components that may mask differences in the spectra of signals generated by objects in different technical conditions. Therefore, it was decided to investigate whether improving the frequency resolution of signal analysis by increasing the resolution would enhance the discriminative properties of the feature vectors. The decomposition of signals with the use of wavelet packets makes it possible to perform such tests.

Wavelet packets are a generalized method of signal decomposition using discrete wavelet transform. In this approach, the subsequent decomposition of the signal can be subjected to both a coarse representation and a detailed representation of the signal. This creates the possibility of analyzing different selected parts of the signal spectrum with higher resolution. A schematic of signal decomposition using wavelet packets, for example at three levels of resolution, is shown in Fig. 10.

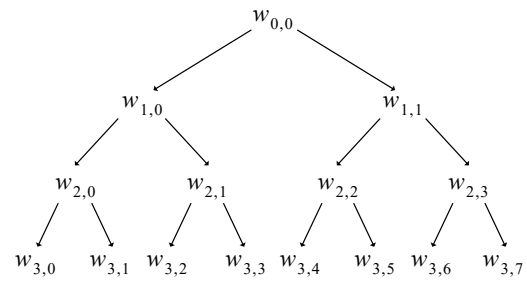


Fig. 10. Signal decomposition scheme using wavelet packets.

The division of the analyzed signal's frequency band corresponding to this decomposition scheme is shown in Fig. 11.

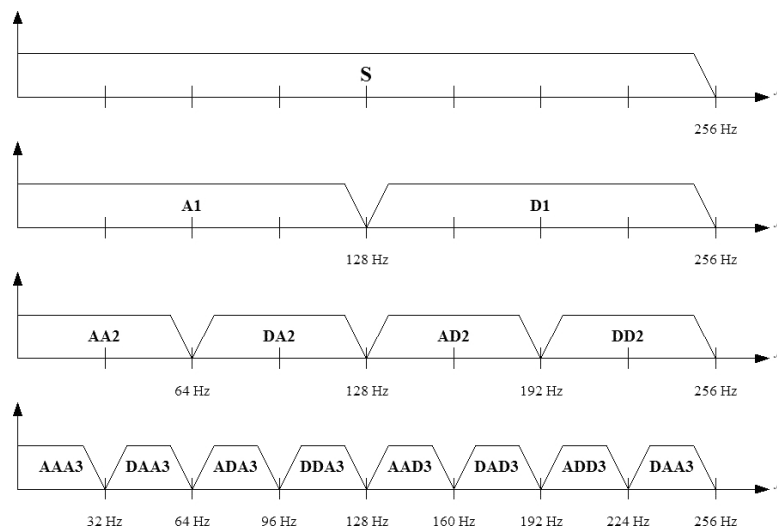


Fig. 11. Division of the signal band as a result of signal decomposition using wavelet packets.

Signal decompositions for the seventh resolution level were performed. The number of decomposition components is  $2^7 = 128$  and the frequency bandwidth of individual decomposition components is  $B_i = 2$  Hz. On the basis of the analysis of the registration spectra (Fig. 5), it should be expected that certain features of the acoustic signal, being a function of the dynamic properties of the seat mechanical system design, will manifest themselves in the frequency range of a few to several tens of Hz. Therefore, limiting the signal analysis to this frequency range allowed us to significantly reduce the number of decomposition components taken into account in further processing. This number was reduced to  $n_{wp} = 26$ .

The method for calculating the values of the individual components of the feature vector remained the same as previously described (Eq. (1)). Also, the signal processing operations, preceding the process of calculating the values of feature vector components, remained unchanged (Fig. 9).

Programming work, related to the implementation of the developed algorithms, was carried out using the MATLAB software platform. An example of the application's interface for signal decomposition using the classical wavelet analysis method is shown in Fig. 12.

The application was designed to support research related to the generation of a feature vector based on acoustic signal recordings produced during the operation of the seat drive device. It includes the last three stages of the feature vector generation process, shown in Fig. 9, i.e., wavelet decomposition, feature extraction, and save feature vector.

The application's input data are digital recordings of acoustic signals, provided as files containing samples of the signal's instantaneous values, after preprocessing (i.e., conversion to uff/txt format, decimation, normalization (Fig. 9)).

Pressing the “get and show” button expands the window to display a list of all registrations contained in the specified directory, indicated by the path. After selecting a registration, the time waveform and signal spectrum are displayed. Additional information, such as sampling frequency, number of registration samples, name of the downloaded file, parameters of the FFT algorithm is also displayed. The spectrum graph can be changed, to highlight important parts by changing some parameters of the FFT algorithm and activating these changes with the “change and show” button.

The main part of the algorithm, after selecting the type of wavelet, is initiated with the decomposition button. As a result, it displays the time waveforms of the reconstructed components for the assumed eight decomposition levels. They illustrate the energy of the signals representing each decomposition level. A graph and a table containing the RMS values of the wavelet coefficient sequences for the selected decomposition levels are also displayed. These values represent the components of the feature vector.

The result of the application is saved to disk in the directory specified by the path in the “folder for saving vector” after pressing the save vector button. Successful completion of this operation is indicated by the green color of the LED indicator.

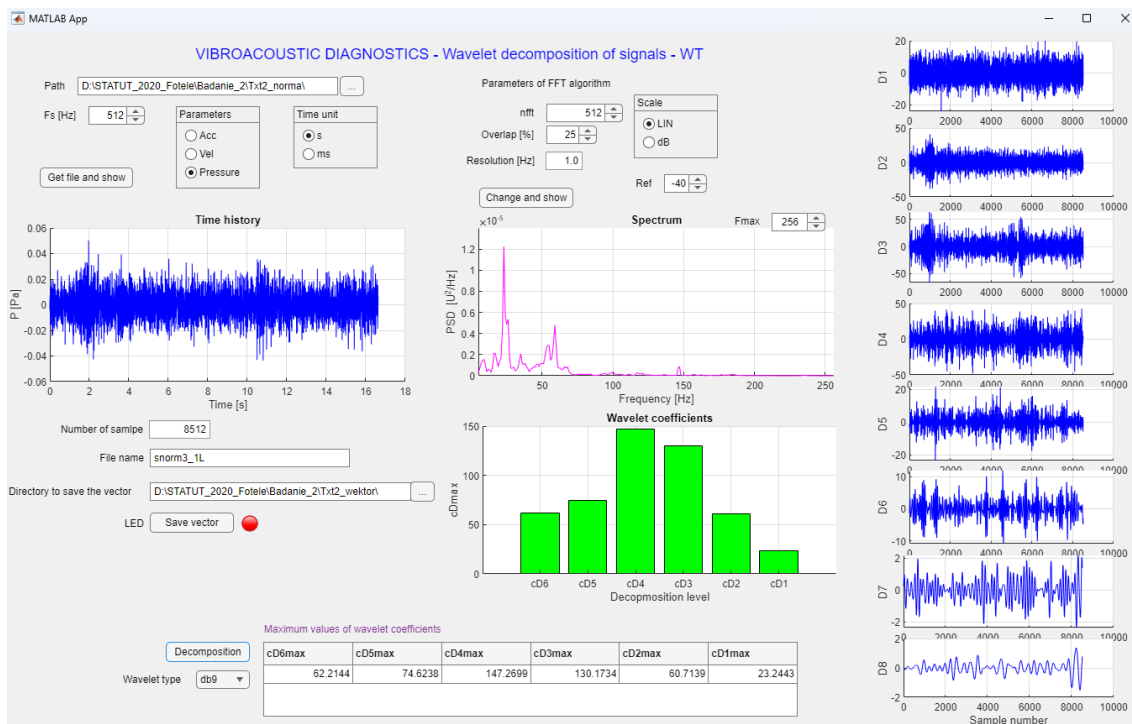


Fig. 12. Appearance of wavelet decomposition application interface.

#### 4. Classification

The described algorithms were used to create sets of feature vectors, which serve as input data for the classification algorithms.

Each component of feature vector can be considered as a coordinate in a space called feature space. In this context, each diagnosed object corresponds to a point in that space called a picture, and a set of objects, belonging to one class corresponds to a certain area encompassing set of their pictures. From the point of view of diagnostics (the recognition process), a desirable situation occurs when, as a result of an appropriate choice of the structure of the feature space, images of objects of different categories occupy disconnected areas. In practice, these areas partially overlap (intermingle), causing diagnostic errors.

To test discriminative properties of the feature vectors we used the “Classification Learner” application available in MATLAB program. This application includes a set of classification algorithms allowing experimental selection of the optimal algorithm for a specific application. The classification results presented below were obtained for the K-nearest neighbor algorithm (for  $K = 3$ ) and decision trees. It should be noted that the final choice of the classification algorithm should be made on a much larger dataset of diagnosed objects, and will most likely differ from the already indicated algorithms. Nevertheless, the obtained results suggest that the feature vectors generated using wavelet analysis of the signal exhibit discriminatory properties, enabling the effective diagnosis of the tested seats.

Due to the small number of tested objects, and the consequently small length of the learning sequence, the testing of particular algorithms included in the

mentioned application was performed according to the method known in the literature as leave-one-out (SOBCZAK, MALINA, 1985). From the set of feature vectors, one feature vector is selected and treated as the test vector. The rest of the set is treated as the learning set. This procedure is repeated for each vector in the set.

Figure 13 shows an example of a scatterplot in feature space for two selected components and the so-called confusion matrix for the learning sequence obtained by classical wavelet analysis.

What draws attention is the grouping of images (points) in the feature space corresponding to damaged objects (blue dots). For this learning sequence, two objects were incorrectly diagnosed, as indicated by the confusion matrix.

For feature vectors generated using wavelet packets, their discriminatory properties were tested with a feature space dimension of  $n_{wp} = 26$ , as already noted.

Figure 14 shows an example of the scatter of points in the feature space, for two selected components and the so-called confusion matrix, for the learning sequence, obtained by analysis using wavelet packets.

The feature space images corresponding to both good and bad objects occupy disjoint areas, although their close proximity may cause misdiagnosis. Qualitatively, the test results are somewhat better than the results of the testing a set of feature vectors obtained with the classical method. In this case, one object was misdiagnosed, as shown in the confusion matrix.

Due to the very small number of test objects and the consequently short length of the learning sequence, no far-reaching conclusions can be drawn from the above results, although they are promising.

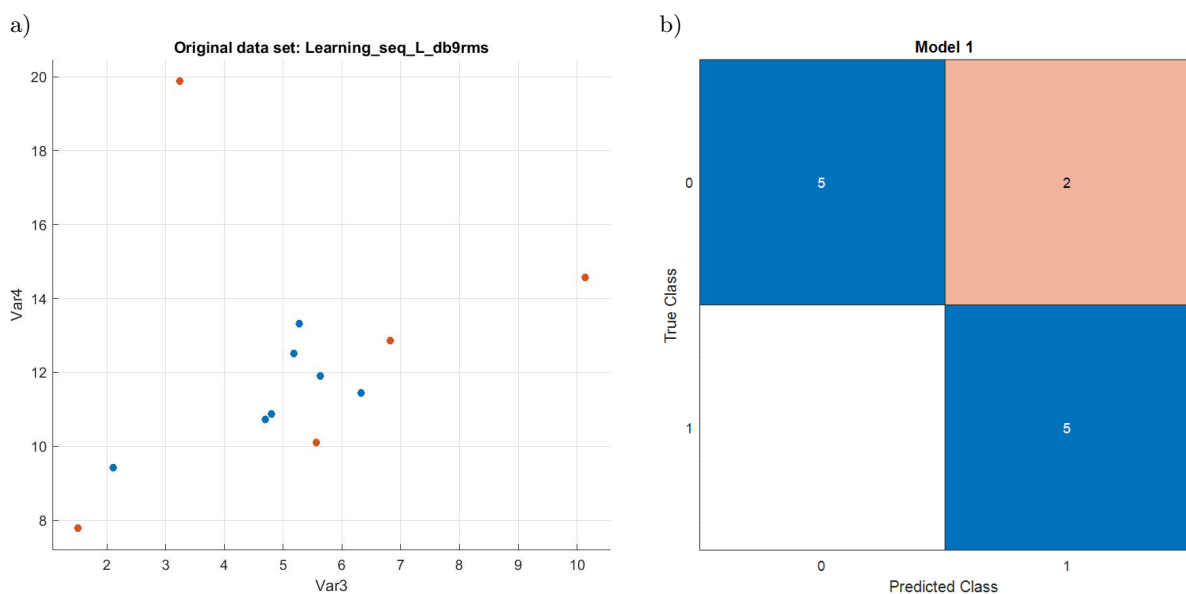


Fig. 13. Results of classical wavelet analysis: a) scatterplot of points in feature space for the two components of the learning sequence; b) confusion matrix.



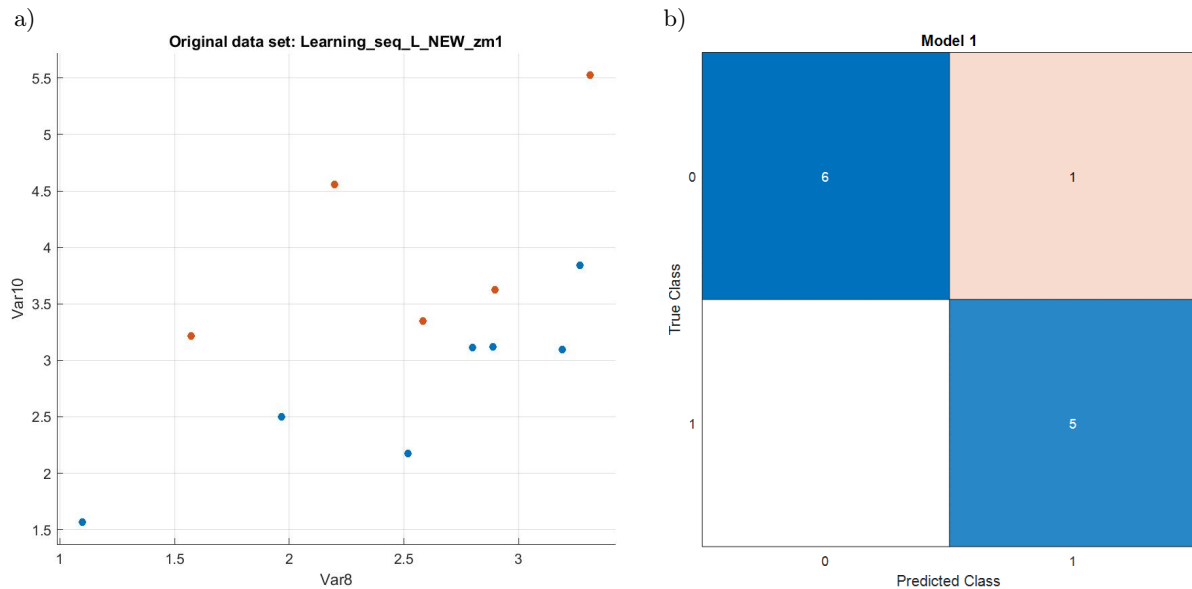


Fig. 14. Results of wavelet packed analysis: a) scatterplot of points in feature space for the two components of the learning sequence; b) confusion matrix.

The small number of research objects was caused by the Coronavirus pandemic and the resulting minimized possibilities of contacts with the seat manufacturer and the successive delayed acquisition of additional research objects. It is assumed that the possibility of accessing a large number of tested seats will soon be restored, allowing for the successive expansion of the measurement database, as was originally planned.

## 5. Conclusions

The obtained results indicate the potential of using wavelet analysis of acoustic signals generated during the operation of the diagnosed mechanical device in technical diagnostics. The feature vectors generated according to the presented algorithms have discriminative properties, allowing for diagnostics of the tested devices using machine learning methods.

As predicted, due to the increased frequency resolution of the diagnostic signal analysis, feature vectors generated using wavelet packets showed better discriminatory properties than those generated using classical wavelet analysis method.

Despite the fact that the obtained results are satisfactory, the effectiveness of the diagnostic method cannot be reliably assessed due to the small number of tested objects. This limitation was caused by objective difficulties.

The research is planned to be continued as originally intended. The machine learning method requires access to a large number of diagnosed objects and the creation, as a result of their research, of a database of diagnostic symptoms (features vectors). Based on these database resources, learning and testing sequences will be created. For optimal selection of

the classifier algorithm and to determine the effectiveness of the developed diagnostic method, it is necessary to use independent learning and testing sequences during testing.

## Acknowledgments

This work was supported by the Ministry of Science and Higher Education of the Republic of Poland (Statutory activity no. 11131020-171).

## References

1. BASZTURA C. (1996), *Acoustical Computer Diagnostic Systems* [in Polish: *Komputerowe Systemy Diagnostyki Akustycznej*], WNT, Warszawa.
2. BATKO W., DĄBROWSKI Z., ENGEL Z., KICIŃSKI J., WEYNA S. (2005), *Modern Methods of Vibroacoustics Processes Research* [in Polish: *Nowoczesne Metody Badania Procesów Wibroakustycznych*], Wydawnictwo Instytutu Technologii Eksploatacji – PIB, Radom.
3. BIAŁASIEWICZ J. (2004), *Wavelets and Approximations* [in Polish: *Falki i Aproksymacje*] WNT, Warszawa.
4. DING L., PENG J., ZHANG X., SONG L. (2023), Sleep snoring sound recognition based on wavelet packet transform, *Archives of Acoustics*, **48**(1): 3–12, doi: [10.24425/aoa.2022.142906](https://doi.org/10.24425/aoa.2022.142906).
5. DUDA R., HART P. (1973), *Pattern Classification and Scene Analysis*, John Wiley & Sons, Inc.
6. GŁOWACZ A. (2014), Diagnostics of synchronous motor based on analysis of acoustic signals with the use of line spectral frequencies and K-nearest neighbor classifier, *Archives of Acoustics*, **39**(2): 189–194, doi: [10.2478/aoa-2014-0022](https://doi.org/10.2478/aoa-2014-0022).

7. HAN X., XU J., SONG S., ZHOU J. (2022), Crack Fault diagnosis of vibration exciter rolling bearing based on genetic algorithm-optimized Morlet wavelet filter and empirical mode decomposition, *International Journal of Distributed Sensor Networks*, **18**(8), doi: [10.1177/15501329221114566](https://doi.org/10.1177/15501329221114566).
8. HUANG W.Y., SOLORZANO M.R. (1971), *Wavelet Preprocessing of Acoustic Signals*, Naval Ocean System Center.
9. International Organization for Standardization (2010), *Acoustics – Determination of sound power levels and sound energy levels of noise sources using sound pressure – Engineering methods for an essentially free field over a reflecting plane* (ISO Standard No. 3744:2010), <https://www.iso.org/standard/52055.html>.
10. LIN J. (2001), Feature extraction of machine sound using wavelet and its application in fault diagnosis, *NDT & E International*, **34**(1): 25–30, doi: [10.1016/S0963-8695\(00\)00025-6](https://doi.org/10.1016/S0963-8695(00)00025-6).
11. LIN J., QU L. (2000), Feature extraction based on Morlet wavelet and its application for mechanical fault diagnosis, *Journal of Sound and Vibration*, **234**(1): 135–148, doi: [10.1006/jsvi.2000.2864](https://doi.org/10.1006/jsvi.2000.2864).
12. MALLAT S.G. (1989), A theory for multiresolution signal decomposition: the wavelet representation, *IEEE Transactions on Pattern Analysis and Machine Intelligence*, **11**(7): 674–693, doi: [10.1109/34.192463](https://doi.org/10.1109/34.192463).
13. PAWLIK P. (2019), The use of the acoustic signal to diagnose machines operated under variable load, *Archives of Acoustics*, **45**(2): 263–270, doi: [10.24425/aoa.2020.133147](https://doi.org/10.24425/aoa.2020.133147).
14. PENG Z.K., CHU F.L. (2004), Application of the wavelet transform in machine condition monitoring and fault diagnostics: A review with bibliography, *Mechanical Systems and Signal Processing*, **18**(2): 199–221, doi: [10.1016/S0888-3270\(03\)00075-X](https://doi.org/10.1016/S0888-3270(03)00075-X).
15. PIERSOL J.S. (1989), *Random Data*, John Wiley & Sons.
16. QIU H., LEE J., LIN J., YU G. (2006), Wavelet filter-based weak signature detection method and its application on rolling element bearing prognostics, *Journal of Sound and Vibration*, **289**(4–5): 1066–1090, doi: [10.1016/j.jsv.2005.03.007](https://doi.org/10.1016/j.jsv.2005.03.007).
17. SOBCZAK W., MALINA W. (1985), *Information Selection and Reduction Methods* [in Polish: *Metody Selekcji i Redukcji Informacji*], WNT, Warszawa.
18. STASZEWSKI W.J. (1998), Wavelet based compression and feature selection for vibration analysis, *Journal of Sound and Vibration*, **211**(5): 735–760, doi: [10.1006/jsvi.1997.1380](https://doi.org/10.1006/jsvi.1997.1380).
19. SUN Q., CHEN P., ZHANG D., XI F. (2004), Pattern recognition for automatic machinery fault diagnosis, *Journal of Vibration and Acoustics*, **126**(2): 307–316, doi: [10.1115/1.1687391](https://doi.org/10.1115/1.1687391).
20. SYED S.H., MURALIDHARAN V. (2022), Feature extraction using discrete wavelet transform for fault classification of planetary gearbox – A comparative study, *Applied Acoustics*, **188**: 108572, doi: [10.1016/j.apacoust.2021.108572](https://doi.org/10.1016/j.apacoust.2021.108572).
21. SZABATIN J. (2000), *Basics of Signal Theory* [in Polish: *Podstawy Teorii Sygnałów*], WKŁ, Warszawa.
22. TANG B., LIU W., SONG T. (2010), Wind turbine fault diagnosis based on Morlet wavelet transformation and Wigner-Ville distribution, *Renewable Energy*, **35**(12): 2862–2866, doi: [10.1016/j.renene.2010.05.012](https://doi.org/10.1016/j.renene.2010.05.012).
23. XI F., SUN Q., KRISHNAPPA G. (1997), Bearing diagnostics based on pattern recognition of statistical parameters, [in:] *5th International Congress on Sound and Vibration*, Adelaide, South Australia.
24. YANG J., ZHOU C., LI X. (2022), Research on fault feature extraction method based on parameter optimized variational mode decomposition and robust independent component analysis, *Coatings*, **12**(3): 419, doi: [10.3390/coatings12030419](https://doi.org/10.3390/coatings12030419).